Cellular and Molecular Biology
E-ISSN : 1165-158X / P-ISSN : 0145-5680
www.cellmolbiol.org
Original Research

Investigation of regulation and mechanism of miR-223 on autophagy of CD4 + T lymphocytes in septic mice

Qi Li[1], Guoan Xiang[2], Chouchun Peng[3], Lixin Xie[4*], WenJie Ji[5*]

[1] Respiratory Department, Chinese PLA General Hospital /Medical School of Chinese PLA
[2] Respiratory Department, The Third Medical Center of Chinese People's Liberation Army General Hospital
[3] Respiratory Department, Pingjin Hospital
[4] Respiratory Department, Chinese PLA General Hospital
[5] Institute of Cardiovascular Disease and Heart Center, Pingjin Hospital

*Correspondence to: xielx301@126.com, ji_wenjie@hotmail.com

Received October 14, 2018; Accepted June 1, 2019; Published August 31, 2019

Doi: http://dx.doi.org/10.14715/cmb/2020.66.7.32

Abstract: T-lymphocyte dysfunction is most important part of immune dysfunction in sepsis, where dynamic change, especially autophagy of CD4+T lymphocytes is found to be related to disease fate. Our study is to i nvestigate the changes of CD4 + T lymphocytes and their autophagy levels in septic miR-223 −/− mouse model injected intraperitoneally with E. coli.120 male C57BL/6J wild-type. Twenty male miR-223 knockout(miR-223-/-) mice were randomly divided into, according to intraperitoneal injection of normal saline (NS) and E. coli solution, normal saline (WT NS) group, sepsis (WT Sep) group, miR-223 −/− NS group and miR-223 −/− Sep group, respectively. The autophagy related protein was monitored with flow cytometry to observe the autophagy of CD4+T lymphocytes. Flow cytometry showed the proportion of CD4 + T lymphocytes in peripheral blood circulation, alveoli, and spleen of mice in the WT Sep group gradually decreased after surgery, the proportion of cells with autophagic activity in this population of cells was significantly higher than that in the WT NS group, and the proportion of CD4 + T lymphocytes with active autophagic activity in miR-223 −/− mice were significantly decreased, but higher than that in the miR-223 −/− NS group and lower than the level of autophagy in CD4 + T cells of wild-type mice. Thus, miR-223 can up-regulate the level of autophagy in CD4 + T lymphocytes of septic mice, suggesting that miR-223 may be used as a potential target for the prevention and treatment of sepsis.

Key words: Sepsis; CD4 + T lymphocytes; Autophagy; Escherichia coli; miR-223.

Introduction

Sepsis is a series of symptoms and signs when infection causes systemic inflammation, organ failure and even death (1). According to the new definition of sepsis given by JAMA in 2016, it is fatal organ dysfunction caused by the host's unregulated response to infection (2). Although fluid resuscitation therapy and the use of antibiotics have made progress in the treatment of sepsis, sepsis is still the leading cause of death in the intensive care unit (ICU). In the body, the most common manifestation of sepsis in the early stage is inflammation. When the inflammation is insufficient, it will not be enough to remove pathogenic microorganisms that invade the body. Excessive inflammation will be the body's self-destructive effect, that is, we often Talking about SIRS or even tissue damage or MODS (3), the body often enters the immunosuppressive stage (4) at the end of its development. This stage is the stage with the highest mortality in patients clinically, because when the patient is in an immunosuppressed state, the chance Pathogenic bacteria will have an opportunity to invade the body (5).

Throughout sepsis, the body's innate and adaptive immune systems play an important role (6). The innate immune system is the first line of defence of the body, mainly including macrophages, neutrophils, dendritic cells, etc. In the specific immune system, the main cell involved in cellular immunity is T lymphocytes. Helper T cells (CD4 + T lymphocytes) play an important role. CD4 + T lymphocytes are highly heterogeneous. According to their surface markers and functional characteristics, they can be divided into several subgroups, the most important of which is the CD4 + helper T lymphocyte (Th) subgroups, which can be divided into Th1, Th2 and th3 subgroups according to their functions and secreted cytokines, Under the action of different cytokines and internal environment, cells can differentiate into four kinds of cells with different functions: Th1, Th2, CD4 + CD25 + regulatory T cells (Treg), and Th17 cells. Th1 cells could secrete IL-2, Interferon – α (IFN-α), interleukin(IL)-12, and IFN- γ and other cytokines, playing an important role in cellular immunity and delayed type hypersensitivity response ,resulting in Th1 response mainly targets the intracellularbacteria and viruses; while Th2 cells secrete IL-4, IL-5, IL-10 and IL-13, which play an important role in humoral immunity; Th3 cells secrete a large number of transforming growth factor (TGF) -β (7).

Autophagy is a normal life activity in cells and is widespread in eukaryotic organisms, and homeostasis in cells requires autophagy (8). Autophagy is a kind of

normal cell function in which macromolecular substance decomposed by degrading abnormal proteins, organelles, etc. in the cell that will be recycled by the cell again. Autophagy is beneficial to the body itself in many cases. When protecting the body from external trauma or pathogen invasion, autophagy can protect the body from the occurrence and development of some diseases to a certain extent, but some special pathological reactions will be formed (9-10).

In some studies, it was found that in the stage of immunosuppression caused by sepsis, T lymphocytes showed abnormal differentiation ability and function, increased apoptosis and so on. So will the autophagy activity of T lymphocytes, especially CD4 + T lymphocytes, which play an important role in sepsis, change to play a role in sepsis?

In this study, we used miR-223 −/− mice to observe the spatial and temporal changes of CD4 + T lymphocytes and the changes in their autophagic activity in a mouse model of sepsis-induced by E. coli and to investigate the regulation of autophagy levels by miR-223 in CD4 + T lymphocytes in a mouse model of sepsis and its mechanism.

Materials and Methods

Animals

Healthy male SPF C57BL/6J mice, 8 – 10 weeks old, weighing 18 – 20 g, were purchased from the Laboratory Animal Center of the Academy of Military Medical Sciences of the Chinese People's Liberation Army under license number SCXK- (Jun) 2012-0004. Healthy male SPF grade miR-223 knockout mice (T002738)B6/JNju-Mir223em1Cd6d359/Nju, miR-223-/y, 8 – 10 weeks old and weighing 18 – 20 g, were purchased from Jiangsu Ji Cui Yao Kang Biotechnology Co., Ltd., and were routinely housed in a clean animal house and subjected to experiments after 1 week of adaptive feeding under a 12 h/12 h light cycle to ensure good ventilation, temperature and humidity.

Experimental methods

The manufacturers of reagents used in this research are shown in Table 1.

Table 1. Experimental reagents.

Reagent	Manufacturers
Escherichia coli strain (ATCC 25922)	Quality control strains of Microbiology
Anhydrous ether	Tianjin Second Chemical Reagent Factory
Ethylenediaminetetraacetic acid (EDTA); Poly-L-Lysine	Sigma Aldrich, USA
7-AAD Viability Staining SolutionPE/Cy7 anti-mouse CD8 Antibody; PE anti-mouse LC3B Antibody; PE/Cy5 anti-mouse CD4 Antibody; FITC anti-mouse CD3 Antibody; Rat IgG2a- PE/Cy5 Antibody; Armenian IgG -PE/Cy7 Antibody; Rat IgG2a – PE Antibody; Rat IgG2b-PE Antibody; Rat IgG2c – FITC Antibody; Cell Staining Buffer	Biolegend, USA
Fetal Bovine Serum(FBS)	Corning, USA
RNAiso Plus	Takara, Japan
Anhydrous formaldehyde solution	Tianjin Chemical Reagent Factory III
Saline	Nanjing Lofu Biotechnology Co., Ltd.
Hematoxylin Stain	Biyuntian Biotechnology Co., Ltd.
Water-soluble eosin stain; Red Cell Lysate	Shanghai Biyuntian Biotechnology Co., Ltd.
Aniline blue	Beijing Bomeide Biotechnology Co., Ltd.

Animal grouping and model preparation

Experimental grouping: 120 male C57BL/6J mice were randomly divided into normal saline (NS) group and sepsis (Sep) group, with 60 mice in each group. Twenty male miR-223 −/− transgenic mice were randomly divided into saline (NS) group and sepsis (SEP) group, with 10 mice in each group.

Preparation of E. coli solution: In this experiment, E. coli solution was prepared using microbiological quality control strain E. coli strain (ATCC25922). E. coli strain was centrifuged at 37 ℃, 1000 r/min, for 5 minutes, the supernatant was discarded and the bacterial pellet was dissolved with sterile saline. The E. coli solution was detected with DensiCHEK-plus instrument with the titer of 2, and the E. coli solution was well prepared for the experiment.

Preparation of model

According to the preparation method of the sepsis animal model, the sepsis mouse model was established by injecting bacteria. In this experiment, septic mice were prepared by intraperitoneal injection of E. coli, and the median lethal dose of E. coli solution was selected according to the previous preliminary experiment. For mice in the SEP group, 0.5 mL of E. coli solution was given to mice with a body weight of 20 g as the baseline, and the volume of intraperitoneal injection was calculated based on the principle that for every 1 g increase in the body weight of mice, the volume of intraperitoneal injection was increased by 0.01 mL. In the NS group, mice were given the same volume of fluid volume of normal saline intraperitoneally to establish model.

Sampling

C57BL/6J mice were sampled at 6 hours, 12 hours, 1, 2, and 3 days after model establishment, and miR-223 −/− mice were sampled at 12 hours and 1 day after intervention. Firstly, 50 μL of peripheral venous blood was collected from the mandibular vein in an ethylene diamine tetraacetic acid (EDTA) anticoagulant tube for flow cytometry of circulating mononuclear cells. Secondly, the mice were sacrificed by exsanguination from the eyeballs after mild anesthesia. Six mice in each group were taken for routine transbronchoalveolar lavage

operation at five-time points, and normal saline precooled to 4 °C was used for lavage. The mice in the lavage group were given transbronchoalveolar lavage with 1 mL precooled sterile normal saline. The above operation was repeated three times continuously to maintain the recovery rate of bronchoalveolar lavage fluid (BALF) at about 90%. After centrifugation of BALF at 4 ° C and 1500 rpm for 10 min, the supernatant was aliquoted and stored at -80 ° C for future use, and the cell mass was resuspended with D-hank's solution for future use. This bronchoalveolar lavage fluid (BALF) was centrifuged and used for flow cytometry analysis. In the non-lavage group, the left lungs of 6 mice were removed for pathological examination. And the spleen, lung, liver, kidney and thymus were removed to calculate the organ index and photographed.

Statistical analysis

Statistical analysis was performed using GraphPad Prism 5.0 software. For those measurement data which met the normality and homogeneity of variance, they were expressed as mean ± standard deviation. The comparison of means was performed by one-way analysis of variance and SNK-q method. For those measure data which did not meet normality or homogeneity of variance, raw data were described in terms of median, interquartile range, and nonparametric rank-sum Mann-Whitney test was used for comparison. Correlations were analyzed using Pearson correlation analysis, with $P < 0.05$ indicating statistical significance.

Results

Body weight changes in mice

Mice in the WT SEP group had an obvious decrease in body weight compared with mice in the WT NS group, with a significant difference in body weight decrease on the 1st day after the intervention (− 1.118 ± 0.1438 g), which continued until the 3rd day.

In mice in the miR-223 −/− SEP group, body weight had been decreased compared with the miR-223 −/− NS group, with a significant difference (− 1.06 ± 0.2159 g) at 12 hours after intervention, which continued until 1st day after intervention. Compared with WT mice, miR-223-/-mice had a significant weight loss earlier after sepsis modeling, indicating that mice with sepsis in miR-223-/-Sep group progressed faster (Figure 1).

Statistics of mouse survival rate

According to the survival rate of WT mice and miR-223-/-mice after modeling, mice in both Sep groups had died, and death occurred earlier in miR-223-/-mice than those in the WT Sep group, moreover, more mice in the miR-223-/-Sep group died than those in the WT Sep group at the same time point; indicating that the sepsis progressed in miR-223-/-mice may progress faster and more severely (figure 2).

Mouse disease score

Pre- and post-intervention health status was scored according to the mouse disease score table (19), as shown in Figure 3.

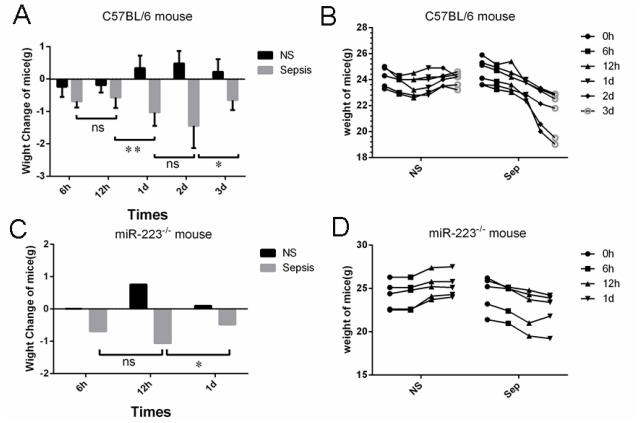

Figure 1. Body weight changes in mice. A: weight change of C57BL/6J mice; Sep mice with the significant weight decrease from day 1 and 2. NS mice weight start to increase from day 1. B: weight change curve of C57BL/6J mice on each time points; no significant change of NS mice weight occur, while gradual weight decrease for Sep mice.C: weight change of miR-223 −/− mice; gradual increase in NS mice, gradual decrease in Sep group, especially on 12h.D: weight change curve of miR-223 −/− mice. Gradual increase in NS group while significant weight decrease on 12h.

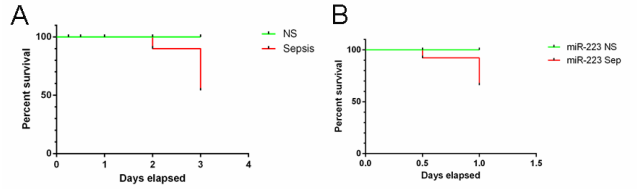

Figure 2. Survival curve of mice after intervention. A: Survival curve of C57BL / 6J mice after the intervention; B: Survival curve of miR-223-/-mice after the intervention.

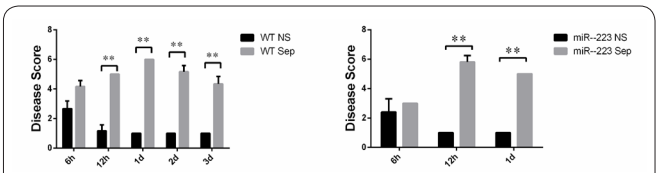

Figure 3. Disease score after intervention in mice.

Spleen index

Calculated statistics according to the spleen index of the mice are shown in the figure4 and figure 5.

Lung index

The lung index results are shown in the figure 6 and figure 7.

Liver index

The hepatic index results are shown in the figure 8.

Renal index

The renal index results are shown in figure 10 and figure 11.

Thymus index

Thymus index results are shown in the figure 12 and 13.

Observation on pathological changes of lung tissues of mice in each group

After HE staining, the pathological changes of lung tissues observed under a common light microscope in

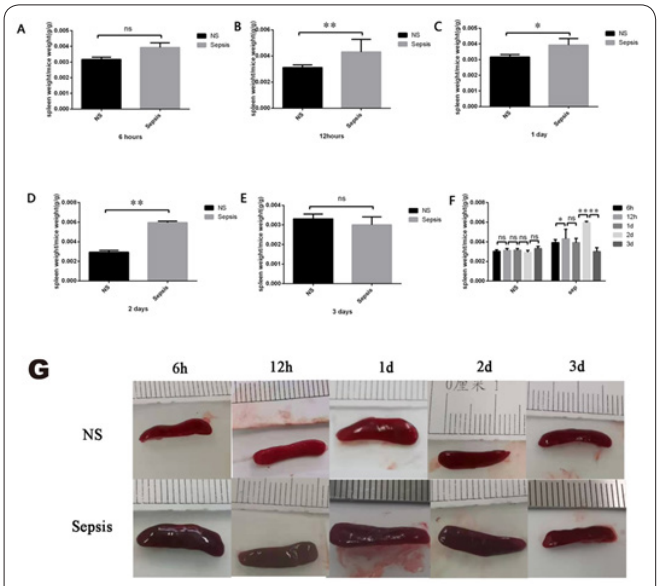

Figure 4. Spleen index after intervention in C57BL/6J mice. A:spleen weight/mice body weight change between NS and Sep mice on 6h;B: spleen weight/mice body weight change between NS and Sep mice on12h;C: spleen weight/mice body weight change between NS and Sep mice on day 1;D: spleen weight/mice body weight change between NS and Sep mice on day 2;E: spleen weight/mice body weight change between NS and Sep mice on day 3;F: Comparison between NS and Sep mice in spleen weight/mice body weight change on each different time points.G: The observation of changes of spleen in deferent groups by naked eye.

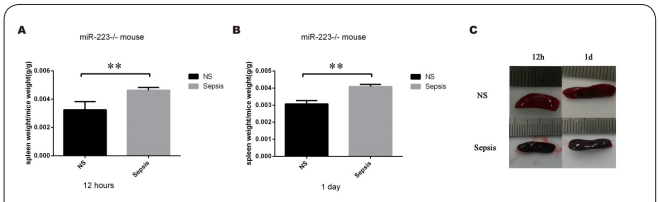

Figure 5. Spleen index after intervention in miR-223 −/− mice .

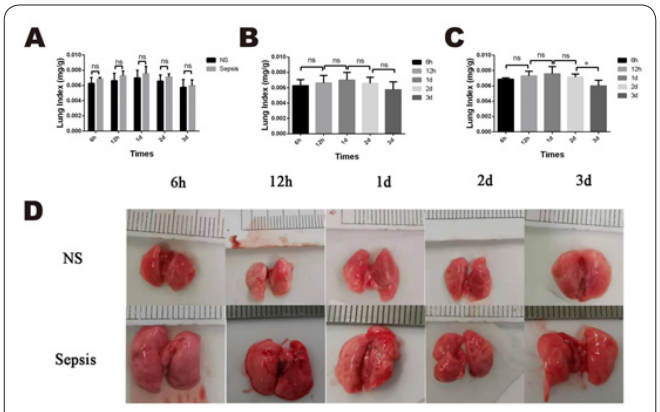

Figure 6. Lung index in C57BL/6J mice. A: Lung index after intervention in C57BL/6J mice; B: Lung index at each time point in the NS group; C: Lung index at each time point in Sep group. D: The observation of changes of lung in deferent groups by naked eye.

each group are shown in Figure 14 and 15. HE staining of lung histopathology at various time points after intervention in C57BL/6J mice Obvious inflammatory cell infiltration was seen in the WT Sep group at 12 hours (shown in Figure 14), and part of the lung septum was thickened. The inflammatory response was significantly increased on the first day, and a large number of inflammatory cell infiltration was seen. The lung tissue struc-

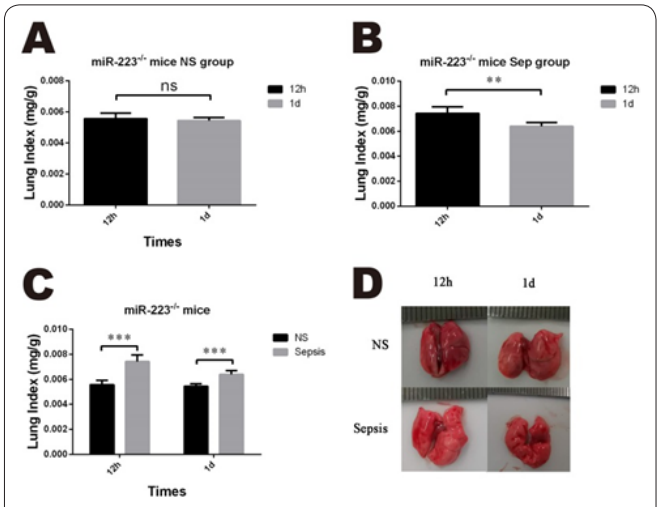

Figure 7. Lung index in miR-223 −/− mice. A: Lung index after intervention in NS group of miR-223 −/− mice; B: Lung index after intervention in Sep group of miR-223 −/− mice; C: Lung index after intervention in miR-223 −/− mice.D: The observation of changes of lung in deferent groups by naked eye.

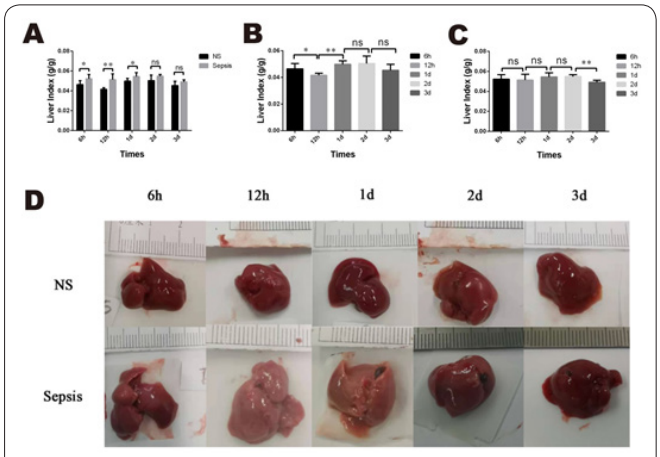

Figure 8. liver index in C57BL/6J mice. A: Liver index of C57BL/6J mice after the intervention; B: Liver index of NS group; C: Liver index of Sep group.D: The observation of changes of liver in deferent groups by naked eye.

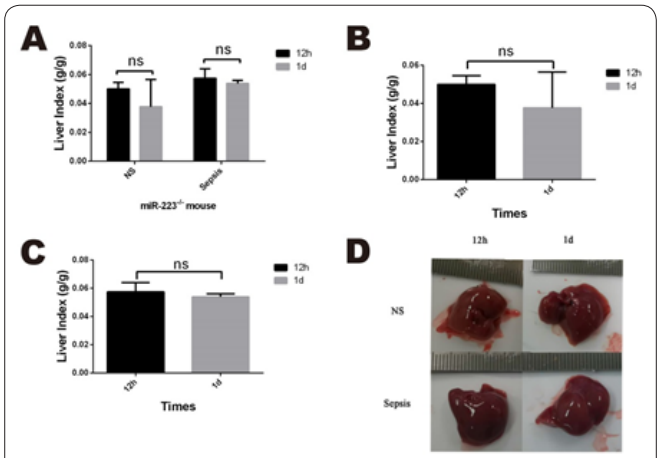

Figure 9. Liver index in miR-223 −/− mice. A : Liver index after intervention in miR-223 −/− mice; B: Liver index in NS group; C: Liver index in Sep group. D: The observation of changes of liver in deferent groups by naked eye.

ture of the miR-223-/- NS group was basically normal; the miR-223-/-Sep group showed obvious inflammatory reaction at 12h (shown in Figure 15), the alveolar sep-

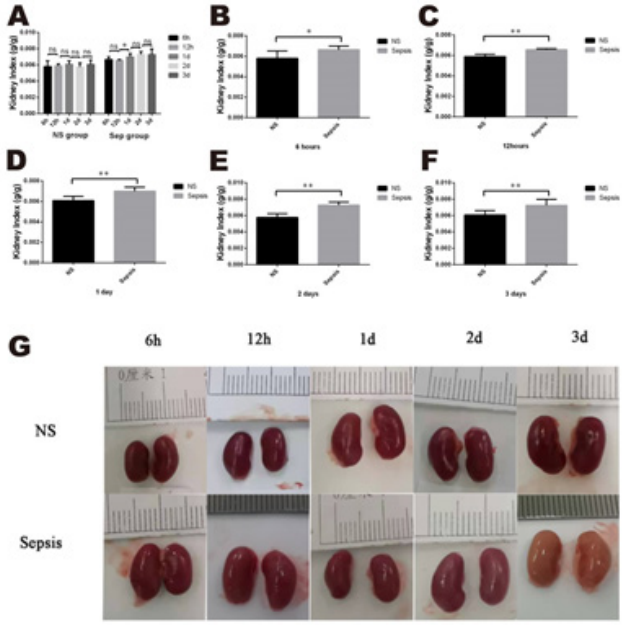

Figure 10. Renal index (kidney weight/mice body weight) after intervention in C57BL/6J mice. A:kidney weight/mice body weight change between NS and Sep mice on 6h; B: kidney weight/mice body weight change between NS and Sep mice on12h; C: kidney weight/mice body weight change between NS and Sep mice on day 1; D: kidney weight/mice body weight change between NS and Sep mice on day 2; E: kidney weight/mice body weight change between NS and Sep mice on day 3; F:Comparison between NS and Sep mice in kidney weight/mice body weight change on each different time points. G: The observation of changes of kidney in deferent groups by naked eye.

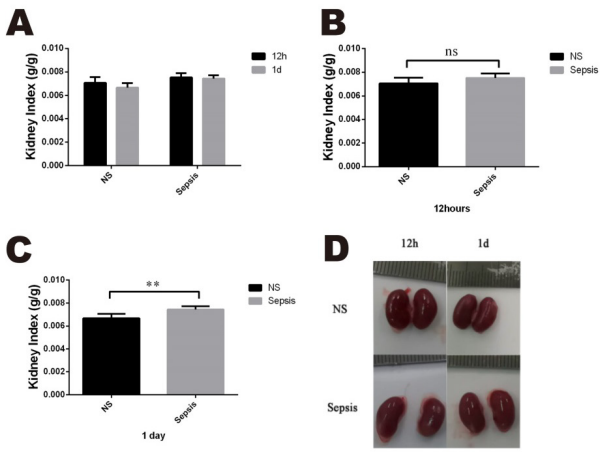

Figure 11. Renal index (kidney weight/mice body weight) after intervention in miR-223 −/− mice. A: Renal index after intervention in miR-223 −/− mice; B: Renal index in NS group; C: Renal index in Sep group; D: The observation of changes of kidney in deferent groups by naked eye.

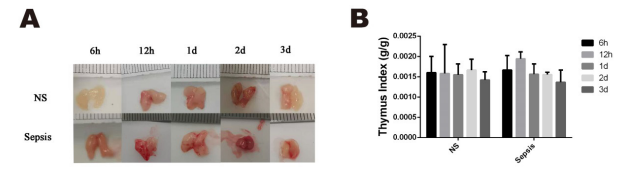

Figure 12. Thymic index after intervention in C57BL/6J mice . A: The observation of changes of thymus in deferent groups by naked eye.B: Comparison between NS and Sep mice in thymus weight/mice body weight change on each different time points.

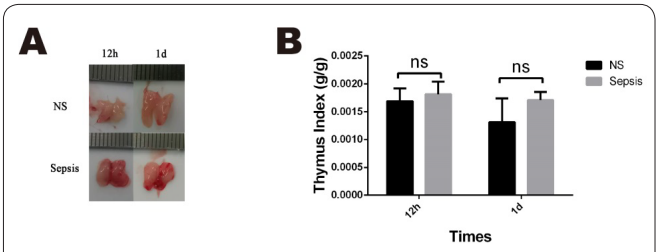

Figure 13. Thymus index after intervention in miR-223 −/− mice. A: The observation of changes of thymus in deferent groups by naked eye. B: Comparison between NS and Sep mice in thymus weight/mice body weight change on each different time points.

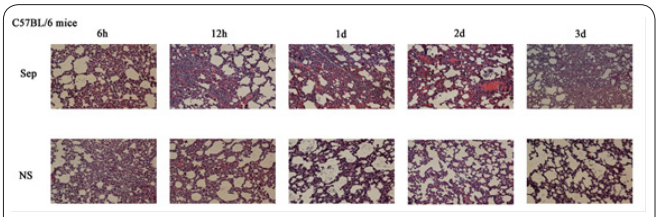

Figure 14. HE staining of lung histopathology at various time points after intervention in C57BL/6J mice .

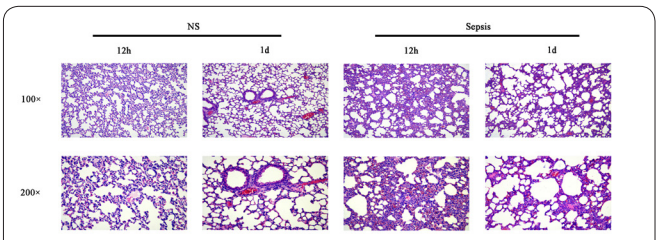

Figure 15. HE staining of lung histopathology at various time points after intervention in miR-223 −/− mice.

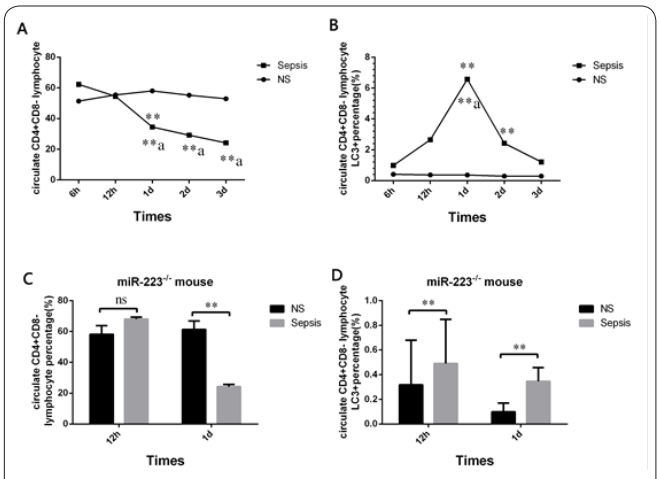

Figure 16. Changes in the proportion of peripheral blood CD4 + T lymphocytes in mice**.** A: Changes in the proportion of peripheral blood CD4 + T lymphocytes in C57BL/6J mice; B: Changes in the level of autophagy in peripheral blood CD4 + T lymphocytes in C57BL/6J mice; C: Changes in the proportion of peripheral blood CD4 + T lymphocytes in miR-223 −/− mice; D: Changes in the level of autophagy in peripheral blood CD4 + T lymphocytes in miR-223 −/− mice. **, p<0.01 vs former time point in the same group. *a, p<0.05 vs the same time point in NS group.**a, p<0.01 vs the same time point in NS group.

tum was obviously thickened, and even the alveolar cavity collapsed, and it was reduced in 1d compared with 12h. The most obvious and worst inflammatory cell infiltration was seen in the WT Sep group at 12 hours, and part of the lung septum was thickened.

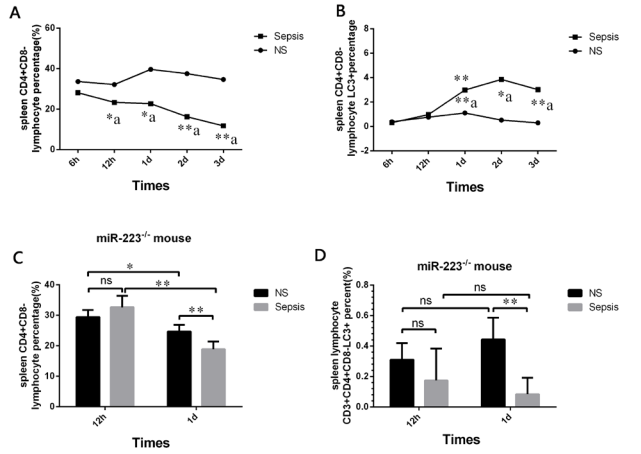

Figure 17. Changes in the proportion of splenic CD4 + T lymphocytes in mice. A: Changes in the proportion of splenic CD4 + T lymphocytes in C57BL/6J mice; B: Changes in the level of autophagy in splenic CD4 + T lymphocytes in C57BL/6J mice; C: Changes in the proportion of splenic CD4 + T lymphocytes in miR-223 −/− mice; D: Changes in the level of autophagy in splenic CD4 + T lymphocytes in miR-223 −/− mice. **, p<0.01 vs former time point in the same group. *a, p<0.05 vs the same time point in NS group.**a, p<0.01 vs the same time point in NS group.

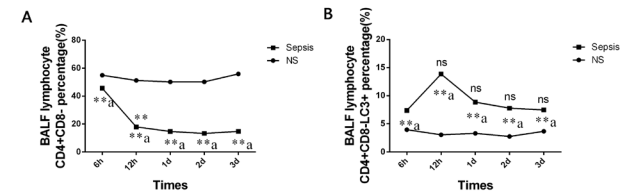

Figure 18. Changes in alveolar CD4 + T lymphocytes in C57BL/6J mice. A: Changes in the proportion of alveolar CD4 + T lymphocytes in C57BL/6J mice; B: Changes in autophagy levels in alveolar CD4 + T lymphocytes in C57BL/6J mice. **, p<0.01 vs former time point in the same group. *a, p<0.05 vs the same time point in NS group.**a, p<0.01 vs the same time point in NS group.

Changes in the proportion of circulating CD4 + T in mice of each group

The change in the proportion of circulating CD4 + T in each group of mice is shown in Figure 16.

Changes in the proportion of splenic CD4 + T in mice of each group

The changes in the proportion of CD4 + T in the spleens of mice in each group are shown in the figure 17.

Changes in the proportion of CD4 + T in the lungs of mice in each group

The changes of CD4 + T ratio in the lungs of mice in each group were shown in the figure 18.

Correlation between circulating CD4 + T lymphocytes and IS in peripheral blood

The proportion of circulating CD4 + T lymphocytes in mice gradually decreased after intervention with E. coli solution. The proportion of CD4 + T lymphocytes and CD4 + T cells undergoing autophagic activity in each group of mice at the same time point was correlated with the IS of the corresponding lung tissue, and the results are shown in the figure 19.

Combined with the results, the microscopic inflammatory changes in the lung tissue of mice in each group and the content of CD4 + T lymphocytes in the bronchoalveolar lavage fluid were changed with the intervention. After E. coli intervention, the CD4 + T cells in the alveoli gradually decreased. The proportion of CD4 + T lymphocytes and CD4 + T cells undergoing autophagic activity in each group of mice at the same time point was correlated with the IS of the corresponding lung tissue, and the results are shown in the figure 20.

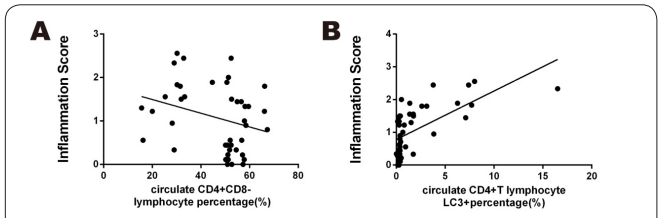

Figure 19. Correlation between circulating CD4 + T lymphocytes and IS in peripheral blood. A: Correlation analysis between the change in the proportion of circulating CD4 + T lymphocytes and the inflammation score; B: Correlation analysis between the change in the proportion of circulating CD4 + T lymphocytes autophagic cells and the inflammation score. Correlation between alveolar CD4 + T lymphocytes and IS.

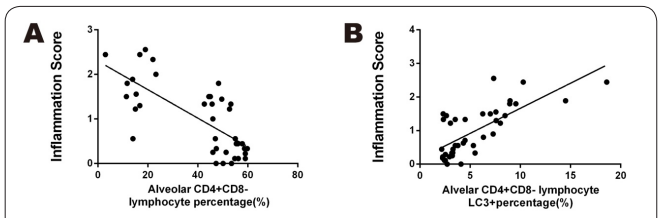

Figure 20. Changes in the proportion of alveolar CD4 + T lymphocytes, autophagic cells of alveolar CD4 + T lymphocytes, and inflammation score. A: Correlation analysis between change in the proportion of alveolar CD4 + T lymphocytes and inflammation score; B: Correlation analysis between change in the proportion of autophagic cells of alveolar CD4 + T lymphocytes and inflammation score.

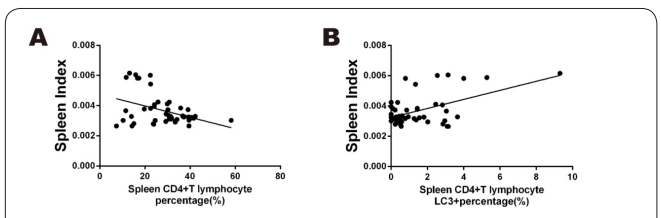

Figure 21. Spleen index and the content of CD4 + T lymphocytes in the spleen of mice. A: Correlation analysis between the change in the proportion of splenic CD4 + T lymphocytes and spleen index; B: Correlation analysis between the change in autophagy level of splenic CD4 + T lymphocytes and spleen index.

Correlation between splenic CD4 + T lymphocytes and splenic index

The results showed that the spleen index and the content of CD4 + T lymphocytes in the spleen of mice in each group were changed with the intervention. After E. coli intervention, the CD4 + T cells in the alveoli gradually decreased. The proportion of CD4 + T lymphocytes and CD4 + T cells undergoing autophagic activity in each group of mice at the same time point was correlated with the IS of the corresponding lung tissue, and the results are shown in the figure 21.

Discussion

Recent studies have found that microRNAs (miRNAs) have an important regulatory role in the process of autophagy. MiRNAs are a class of evolutionarily conserved non-coding small RNAs that can regulate the expression of target genes at the post-transcriptional level and participate in many important cellular biological processes. In the process of autophagy, miRNAs are more mainly involved in the regulation of the core pathway of autophagy in addition to regulating the upstream signaling network of autophagy and affecting the level of post-translational modification of certain autophagy-related proteins. Whether alone or as a member of the entire gene cluster, the expression of miRNAs affects the occurrence and development of diseases through autophagy to regulate inflammatory responses, immune status, and cell death. More meaningfully, recent studies have found that miRNAs affect the survival of T lymphocytes through autophagy (11-12).

In the mouse experiment, through the description of body weight change curve, survival rate and mouse disease score, it can be seen that the sepsis model in this experiment was successful. And a series of observations and organ index assessments were performed for the thymus, lung, liver and spleen, which provided a comprehensive summary of "clinical manifestations" and "signs" of the sepsis model in this experiment. According to the calculation, statistical analysis and visual observation of organ index of spleen, lung, liver, kidney and thymus, it could be seen that intraperitoneal injection of normal saline was a stimulus to mice, but the stimulus was small, causing only transient discomfort and manifestation to mice, and then returned to normal. Intraperitoneal injection of E. coli is not a small stimulus to mice, resulting in sepsis with systemic inflammatory response characterized by multiple organ involvement. As an important site of immune system involvement and rich in various inflammatory cells, we selected the lung, spleen, thymus, liver and kidney as the organs for observation, scored the disease grade of mice by observing the health status before and after the stimulus, reflected the overall health status of mice indirectly by the measurement of mouse body weight, and finally saw the prognosis of mouse sepsis model established in this experiment according to the survival curve. In the C57BL/6J mouse sepsis (Sep) group, 12 hours and 1 day after intervention were the disease turning points of the sepsis model established in this experiment. And according to the statistics of organ index, each organ indexpeaked at 1 day after intervention. At this time, the mice showed depression, rough hair, white transparent viscous secretions in the corners of the eyes, and even hunched head buried and shortness of breath. The overall situation of miR-223 −/− mice progressed more rapidly than that of C57BL/6J mice, the characteristics of organ injury were more obvious, and the induced sepsis mouse model was more severe.

The results of a "multi-spatiotemporal" study using flow cytometry to study the autophagy level of CD4 + T lymphocytes in septic mice showed that the proportion of CD4 + T lymphocytes in peripheral blood circulation, spleen and lung of mice decreased after E. coli intervention, while the CD4 + T lymphocytes with autophagy increased significantly after E. coli intervention, and then gradually decreased, which indicated that in the disease process of sepsis, pathogenic bacteria promoted the autophagy of CD4 + T lymphocytes, and then T lymphocyte autophagy led to active programmed cell death, which played an important role in sepsis immunosuppression. In this experiment, it could also be seen that the sudden decrease of CD4 + T lymphocytes directly affected the disease score of mice, resulting in a sudden decrease in body temperature, touch and systemic inflammatory response in mice. We can therefore speculate that loss of miR-223 may lead to a decrease in overall CD4 + T lymphocytes in mice, and also affect the autophagic activity of CD4 + T lymphocytes, which leads to increased mortality and poor prognosis in mice (13).

In this experiment, it was found that in the mouse model of sepsis, T lymphocytes (including CD4 + T lymphocytes, CD8 + T lymphocytes) showed decreased activity and increased death, resulting in immunosuppression in the animal model of sepsis. While in miR-223 −/− mice, their CD4 + T lymphocyte autophagic activity was found to be abnormal, the sepsis model in miR-223 −/− mice progressed faster and more severely. Adaptive immunosuppression caused by autophagy further affected the activation of non-targeted immunity (host immunity), released more inflammatory cytokines, and further aggravated the abnormal function of autophagy response, which in turn accelerated T lymphocyte death and led to more severe immunosuppression, entered a vicious cycle, and finally led to the death of sepsis model animals.

According to a large amount of data from the experiment, we found that the abnormal expression of miR-223 can affect the normal differentiation or even proliferation of cells, or even the normal function of cells. It has been experimentally confirmed that miR-223 is a protective factor in a mouse model of diet-induced insulin resistance type II diabetes, and deletion of miR-223 leads to more severe adipose inflammation and abnormal polarization of macrophages, which can only appear uniformly as M1 type (14-15). In a mouse stroke model, miR-223 –/– transgenic mice were found to have a higher number of brain cell deaths and a higher probability of systemic ischemia due to the intervention of excitotoxic substances. It can be seen that miR-223 is a protective factor in neural cells from damage stimulated by external factors. In a mouse model of experimental autoimmune encephalomyelitis (EAE), miR-223 is a risk factor for overwhelming pathogenic Th17 T lymphocyte differentiation of primitive T lymphocytes. MiR-223 depletion also affects the activation and differentiation of dendritic cells, while the activation of dendritic cells affects the initial stage of T lymphocyte differentiation (16). FOXO1 also plays an important role in the activation and self-renewal of T cells (17).

As one of the key molecules regulating sepsis, tumor necrosis factor (TNF), which promotes inflammation, and the pathways it is involved can be regulated and targeted by a variety of microRNAs. It has been found that miR-155 expression is enhanced in macrophages and liver tissues intervened by lipopolysaccharide (LPS) and tumor necrosis factor (TNF), which affects the prognosis of the disease by regulating the number of tumor

necrosis factor receptor-1 (TNFR1). Among them, lipopolysaccharide (LPS), as a major component of the cell wall of Gram-negative bacteria, can elicit TLR4 activity, allowing TLR4 signaling to regulate multiple microRNAs in cells involving innate immunity. In the meantime, FOXO1 ameliorates the progression of inflammatory bowel disease by reducing the damage of intestinal mucosal tissue through the regulation of TLR4/MyD88/MD2-NF-κB pathway in a mouse model of inflammatory bowel disease (18-19). Elevated TLR4 expression in airway epithelium affects T lymphocyte differentiation in asthmatic airway inflammation. Acute chorioamnionitis will lead to increased expression of miR-223 in fetal organs, thus demonstrating that FOXO1 can be regulated by miR-223 as a target gene (20). Transcription factors are key to T cell failure and are also important for effector and memory T cells. FOXO1 is one of the important transcription factors affecting T failure (21). When stimulated by T lymphocyte receptors (TCRs), etc., CD4+ T lymphocyte activation requires energy supply through autophagy-dependent lysosomal breakdown pathways to maintain their functional stability. In addition, recent studies have found that autophagy also depends on connexin p62 degradation to change the amount of Bcl-10 to further regulate the activation of NF-κB pathway by TCR signaling, ultimately affecting the activation of T lymphocytes (22). Therefore, miR-223 may regulate autophagic activity by regulating FOXO1 expression and further affecting NF-κB pathway activation.

As the disease progresses in septic mice, it will induce depletion of CD4 + T lymphocytes and enhance autophagic activity. While the loss of miR-223 leads to faster and more severe sepsis due to inhibition of autophagic activity in CD4 + T lymphocytes. MiR-223 acts by regulating FOXO1 expression to affect changes in autophagic activity in septic CD4 + T lymphocytes. The effect of miR-223 on autophagy in CD4 + T lymphocytes can be intervened to establish an experimental and theoretical basis for targeted immunotherapy of sepsis.

AcknowledgementS

Grants from the National Natural Science Foundation of China, Grant No. 81670005.

Interest conflict

None.

Author's contribution

All work was done by the author named in this article and the authors accept all liability resulting from claims which relate to this article and its contents. Qi Li, Guoan Xiang and Chouchun Peng collected and analysed the data; Qi Li wrote the text and all authors have read and approved the text before publication; Lixin Xie and WenJie Ji contributed equally to this work as the co-first author; Lixin Xie and WenJie Ji are the co-corresponding authors.

References

1. Patricia P, José AP, Luís MB. Immune response in bacterial and candida sepsis. Eur J Microbiol Immun 2009; 9(10): 1-9.

2. Donnelly JP, Safford MM, Shapiro NL , Baddley JW, Wang HE. Application of the third international consensus definitions for sepsis (sepsis-3) classification: a retrospective population-based cohort study. Lancet Infect Dis 2007; 17(6): 661-670;

3. Delano MJ, Ward PA. Sepsis-induced immune dysfunction: can immune therapies reduce mortality. J Clin Invest 2016; 126(1): 23-31.

4. Hamers L, Kox M, Pickkers P. Sepsis-induced immunoparalysis: mechanisms, markers, and treatment options. Minerva Anestesiol 2015; 81(4): 426-39.

5. Jia L, Ming L, Longxiang S, Huijuan W, Kun X, Jie D, et al. Alterations of T helper lymphocyte subpopulations in sepsis, severe sepsis, and septic shock: a prospective observational study. Inflammation 2015; 38(3): 995-1002.

6.Parzych KR, Klionsky DJ. An overview of autophagy: morphology, mechanism, and regulation. Antioxid Redox Sign 2014; 20: 460-473.

7. Richard SH, Kevin WT, Paul ES, Robert ES, Jia JH, Katherine CC, et al. Sepsis-induced apoptosis causes progressive profound depletion of B and CD4+ T lymphocytes in humans. J Immunol 2001; 166(11): 6952-6963

8.Yorimitsu T, Klionsky DJ. Autophagy: molecular machinery for self-eating. Cell Death Differ 2005; 12(Suppl 2): 1542-1552.

9.Levine B, Kroemer G. Autophagy in the Pathogenesis of Disease. Cell 2008; 132: 0-42.

10.Fabian B, Christoph R, David VC, Mihael V, Jérémie G, Alexander K, et al. U6 is unsuitable for normalization of serum miRNA levels in patients with sepsis or liver fibrosis. Exp Mol Med 2013; 45: e42.

11.Mott JL, Kobayashi S, Bronk SF. MiR-29 regulates Mcl-1 protein expression and apoptosis. Oncogene 2007; 26: 6133-6140.

12. Pascal P, Stefano V, Katherine M, Agnès M, Carlo B, Benoît, et al. miR-221 overexpression contributes to liver tumorigenesis. Proc Natl Acad Sci U S A 2010; 107: 264-269.

13. Huijuan W, Pengjun Z, Weijun C, Dan F, Yanhong J, Lixin X. Serum microRNA signatures identified by Solexa sequencing predict sepsis patients' mortality: a prospective observational study. PLoS One 2012; 7: e38885.

14. Magali F, Xavier T, Cécile G, Eric P, Dominique CH, Christophe R, et al. Identification of restricted subsets of mature microRNA abnormally expressed in inactive colonic mucosa of patients with inflammatory bowel disease. PLoS One 2010; 5: e13160.

15.Shiqi Huang, Yani Wei, Yuchuan Zhao. Therapeutic Effect of Total Flavonoid of Spatholobus suberectus Dunn on Escherichia coli Sepsis, China Animal Husbandry & Veterinary Medicine 2019; 46: 297-306.

16. Haneklaus M, Gerlic M, Neill1 LAJO, Masters SL. MiR-223: Infection, inflammation and cancer. J Intern Med 2013; 274: 215-226.

17.Lu H, Buchan RJ, Cook SA. MicroRNA-223 regulates Glut4 expression and cardiomyocyte glucose metabolism. Cardiovasc Res 2010; 86: 410-420.

18. Tiffany S, Bo L, Xiaolei T, Jidong X, Weirong X, Weixing S, et al. MicroRNA223 promotes pathogenic T-cell development and autoimmune inflammation in central nervous system in mice. Immunology 2016; 148: 326-338.

19.Marcel N, Hedrick SM. A key control point in the T cell response to chronic infection and neoplasia: FOXO1. Curr Opin Immunol 2020; 63: 51-60.

20.Fan, WuQiang, Morinaga, Hidetaka, Kim, Jane J, et al. FoxO1 regulates Tlr4 inflammatory pathway signalling in macrophages. Embo Journal 2010; 29: 4223-4236.

21. JoonHo L, Chong JK, Jung-Sun K, Deug-Chan L, Sejin A, Bo HY. Increased miR-223 expression in foetal organs is a signature of acute chorioamnionitis with systemic consequences. J Cell Mol Med 2018; 22: 1179-1189.

22.PauL S, Kashyap AK, Jia W, He YW, Schaefer BC. Selective autophagy of the adaptor protein Bcl10 moduLates T cell receptor activation of NF-kappaB. Immunity 2012; 36: 947-958.